Effective Doping and Suppression of Fermi Surface Reconstruction via Fe Vacancy Disorder in K_{x}Fe_{2-y}Se_{2}

Tom Berlijn, P. J. Hirschfeld, and Wei Ku (□□)

Phys. Rev. Lett. **109**, 147003 — Published 3 October 2012

DOI: 10.1103/PhysRevLett.109.147003

Effective doping and suppression of Fermi surface reconstruction via Fe vacancy disorder in $K_xFe_{2-y}Se_2$

Tom Berlijn,[1] P. J. Hirschfeld,[2] and Wei Ku(顧威)[1,3]

[1]*Condensed Matter Physics and Materials Science Department, Brookhaven National Laboratory, Upton, New York 11973, USA*
[2]*Department of Physics, University of Florida*
[3]*Physics Department, State University of New York, Stony Brook, New York 11790, USA*

We investigate the effect of disordered vacancies on the normal-state electronic structure of the newly discovered alkali-intercalated iron selenide superconductors. To this end we use a recently developed Wannier function based method to calculate from first principles the configuration-averaged spectral function $\langle A(k,\omega)\rangle$ of $K_{0.8}Fe_{1.6}Se_2$ with disordered Fe and K vacancies. We find that the disorder can suppress the expected Fermi surface reconstruction without completely destroying the Fermi surface. More interestingly, the disorder effect raises the chemical potential significantly, giving enlarged electron pockets similar to highly doped KFe_2Se_2, without adding carriers to the system.

PACS numbers: 74.70.-b, 71.15.-m, 71.18.+y, 71.23.-k

The newly discovered [1] alkali-intercalated iron selenide selenide superconductors $A_xFe_{2-y}Se_2$, with A=K, Rb, Cs, share a set of properties that distinguish them from any of the other iron based superconductor(FeSC) families. Their transition temperature is found to be as high as $T_c = 31$K at ambient pressure [1], high in comparison with the other 11-type chalgogenides. They are the first FeSC on the verge of becoming an antiferromagnetic (AFM) insulator [2]. The (AFM) order has a novel block type structure, as was predicted from DFT [32] and observed by neutron diffraction [3], with an unprecedented high transition temperature of $T_N = 559$K and magnetic moment of $3.31\mu_B$/Fe. From ARPES experiments [4–10], only electron pockets are found and no hole pockets, seemingly ruling out the popular $s^{\pm}$ pairing scenario [11]. Last, but from an electronic structure point of view certainly not least, they contain significant numbers ($\sim 20\%$) of Fe and K vacancies (V_{Fe} and V_K).

While the presence of these vacancies has been well accepted, their distribution is currently under debate. From the superlattice peaks in neutron diffraction studies [3] it is concluded that the Fe vacancies form a $\sqrt{5}\times\sqrt{5}$ superlattice with strong long-range order. On the other hand, a different scenario has been suggested for those samples which display simultaneously long range magnetic order and superconductivity, namely that of a phase separation, whereby the ordered Fe vacancies only exist in one of the phases. Some scanning tunneling microscopy [12], nuclear magnetic resonance [13], and transmission electron microscopy (TEM) measurements [14] conclude that the second phase contains no Fe vacancies. Other TEM [4, 15] and x-ray absorption near edge structure measurements [16] conclude that the second phase contains disordered Fe vacancies.

An obvious puzzle emerges immediately upon examining angle-resolved photoemission spectroscopy (ARPES) measurements [4–10]. As was demonstrated theoretically [17], the $\sqrt{5}\times\sqrt{5}$ superlattice of Fe vacancies must induce a strong reconstruction of the Fermi surface and the band structure, due to the huge scattering associated with the vacancy. However, current ARPES results all show a simple electronic structure without any indication of reconstruction. A possible solution [17] to this puzzle is that the regions to which ARPES measurements are sensitive must contain poorly ordered Fe vacancies. Earlier DFT calculations [32–34] have established that the vacancy ordered regions will open a magnetic gap such that they cannot contribute to the band structures near the Fermi surface, regardless their volume fraction. This explanation, however, is vulnerable to the potential problem that while vacancy disorder might suppress the band structure reconstruction, it may also destroy completely the Fermi surface. It is thus timely to examine the physical effects of Fe vacancy disorder in this class of materials.

The ARPES experiments also reveal a peculiar behavior of the $A_xFe_{2-y}Se_2$ family. Regardless of the nominal value of x and y, the observed Fermi surfaces always contains large electron pockets in the zone corner, as if the system is strongly electron doped compared to the "245" parent compound $A_{0.8}Fe_{1.6}Se_2$. In fact, the chemical potential is shifted so much that not only do the hole pockets at the zone center submerge entirely below the chemical potential, but also a small electron pocket appears instead. Consequently, these systems are commonly regarded as strongly electron doped, closer to $A_1Fe_2Se_2$ (122) than 245. However, complementary energy dispersive x-ray spectroscopy measurements find the composition to be close to 245 instead. In particular in [4, 10] the compositions have been found to be nearly perfect 245, implying that there are simply not enough Fe atoms to constitute a non-negligible amount of volume fraction of the 122 structure. This raises the question as to what the origin of the large electron doping could be.

Considering the essential role of doping in the magnetism and superconductivity of these materials, a physical explanation of this peculiar behavior is clearly of highest importance.

In this Letter, we address these two important issues by studying the influence of vacancy disorder on the alkali-intercalated Fe selenides, using a recently developed Wannier function based method to calculate from first principles the configuration-averaged spectral function $\langle A(k,\omega)\rangle$ of $K_{0.8}Fe_{1.6}Se_2$ with disordered Fe and K vacancies. We find that the disorder does indeed suppress the band structure reconstruction without completely destroying the Fermi surface. Furthermore, we find that the disorder raises the chemical potential significantly, eliminating the hole pockets and enlarging the electron pockets, in excellent agreement with the ARPES experiments, *without* adding carriers. We provide a microscopic explanation for the origin of the effective doping in terms of the disorder induced frequency broadenings of the bands. In addition, we find the emergence of strongly incoherent carriers. Our result demonstrates clearly the general inapplicability of Luttinger theorem in disordered systems, and suggests an alternative interpretation of existing ARPES measurements.

The band structure of a disordered system is given by the configuration-averaged spectral function: $\langle A_n(k,\omega)\rangle = \sum_c P^c A_n^c(k,\omega)$ of Wannier orbital [18] n, crystal momentum k and frequency ω, in which configuration c is weighted by its probability P^c. By treating the disordered configurations within the supercell approximation, their spectral functions $A_n^c(k,\omega)$ can be obtained directly from the supercell eigenvectors and eigenvalues, using the unfolding method [19]. To handle the computational cost related to the large sizes of the supercells, essential for a proper treatment of the disorder, we employ the recently developed Wannier function based effective Hamiltonian method [20]. The low energy Hilbert space is taken in [-6,2]eV consisting of the Wannier orbitals of Fe-d and Se-p characters. The influence of the Fe and K vacancies is extracted from three DFT [21] calculations: the clean KFe_2Se_2 and the single vacancy supercells $K_7Fe_{16}Se_{16}$ and $K_8Fe_{15}Se_{16}$. For the configurational average, we use 10 large supercells (e.g. Fig.1(b)) of random size, shape and orientation containing 176 atoms on average, and assume an equal probability among the configurations. Benchmarks demonstrating the high accuracy of the effective Hamiltonian method and the convergence of the configuration average against the size and the number of configurations are given in Ref. [21].

As a reference, let's first re-examine the fully $\sqrt{5}\times\sqrt{5}$ ordered 245 system that shows strong band structure reconstruction [17]. To facilitate the comparison with ARPES, Figure 1(c) shows the band structures and Fermi surfaces in the 1-Fe Brillouin zone (c.f. Fig. 1(a)). Indeed, the lower panel shows a very strong reconstruction of the Fermi surface that bears no resemblance to the observed ARPES measurements [4–10]. This strong Fermi surface reconstruction is not a special property of the $\sqrt{5}\times\sqrt{5}$ ordering, but expected to happen for other vacancy orderings [14, 15] in general, due to the very strong scattering against the Fe vacancies. The top panel also shows that the whole band structure, not just the Fermi surface, is reconstructed, with gap openings and complex folded features occurring everywhere in both Fe and Se bands. For example, the red bars in the middle panel indicate two large gap opening on the order of 300-400 meV. These kinds of strong reconstructions should in principle allow ARPES to quantify the strength of the vacancy order, including the semiconducting samples that exhibit no Fermi surface. The fact that no such reconstruction has been reported is at odds with the strong vacancy order observed by neutron scattering [3].

The configuration-averaged spectral function in Fig. 1(d) confirms that strong disorder in the vacancies introduces very large incoherent scatterings. The Fe bands now develop large line widths in both momentum and frequency, reflecting their short mean free path and lifetime. More dramatically, the top of the Se bands within [-4,-2]eV even becomes unrecognizable, due to the large repulsive potential of ∼0.6eV/0.2eV from Fe/K vacancies on their 4/8 neighboring Se orbitals. Nevertheless, even for such a completely disordered case, Fig. 1(d) shows that the Fe band structure and the Fermi surface survive the strong vacancy disorder effects, displaying the characteristics of a dispersive band structure. On the other hand, Fig. 1(d) shows the clear suppression of the reconstruction in the band structure and the Fermi surface. All the gap openings and folded features are washed out. In fact, other than the strong broadening effects and a clear reduction of bandwidth, the resulting band structure and Fermi surfaces agree very well with those of the clean 122 system in Fig. 1(e). We have thus provided quantitative support to the notion that the regions to which ARPES measurements are sensitive must contain poorly ordered Fe vacancies.

Figure 1(d) also shows an unexpected effect of the vacancy disorder, namely a large shift of the chemical potential. Indeed, the chemical potential is now ∼200meV above the tip of the hole pockets, and allows a small electron pocket to appear around the Z point. Correspondingly, the electron pockets at the X/R point are much larger than the parent compounds of all families of Fe-based superconductors. In fact, the resulting Fermi surface looks very much like that of the heavily doped 122 system in Fig. 1(e), even though the system actually contains *no* additional electrons. Specifically, the significant sinking of the hole pockets in our result is in excellent agreement with the ARPES measurements, in great contrast to the near toughing to the Fermi surface of the hole pockets in the 122 case (c.f. Fig. 1(e) and [30]). Obviously, a Luttinger count from the volume of the Fermi surface would give the illusion of heavy electron doping

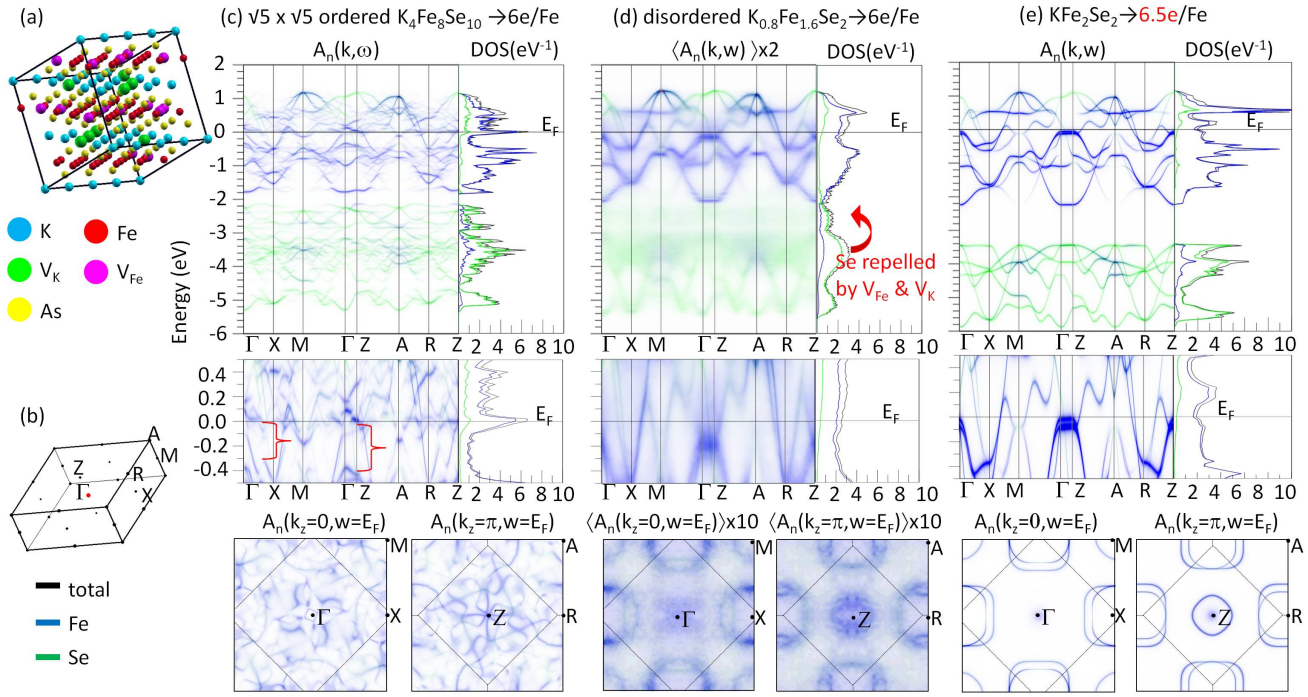

FIG. 1: (color online) (a) An example of a large sized supercell used for the configurational average and (b) 1-Fe Brillouin zone. Band structure, density of states and Fermi surface of $\sqrt{5}\times\sqrt{5}$ ordered Fe and K vacancies(c), disordered $K_{0.8}Fe_{1.6}Se_2$(d) and KFe_2Se_2(d). The dashed lines in the Fermi surface plots mark the 2-Fe Brillouin zone boundaries. The band structure and Fermi surface of the disordered $K_{0.8}Fe_{1.6}Se_2$ are enhanced by a factor of 2 and 10 respectively for better visualization.

for this undoped system. This is a clear demonstration that Luttinger theorem should never be applied to systems with strong disorder [22, 23]. Specifically in this case, our result suggests that the experimental samples showing 122 like Fermi surface might not even be doped at all.

Microscopically, this strong shift of chemical potential (or an *effective* "doping") is to be distinguished from real doping, for example in the case of Co substituted $BaFe_2As_2$, in which the chemical potential shift is a direct consequence of the additional valence electron in the system [23]. (This conclusion differs from the previous studies [24, 25]). Figure 2(a) reveals more insight by ignoring the impurity potential in the calculation (but still removing Fe orbitals at the disordered vacancy sites). In this case, the effective doping becomes negligible, as an "expected" chemical potential of an undoped system is found, giving both hole and electron pockets of regular sizes. On the other hand, an average account of the impurity potential via the virtual crystal approximation (c.f. Fig. 2(b)) misses entirely the effective doping as well. Therefore, the strong chemical potential shift is only realized from the disordered nature of the impurity potential.

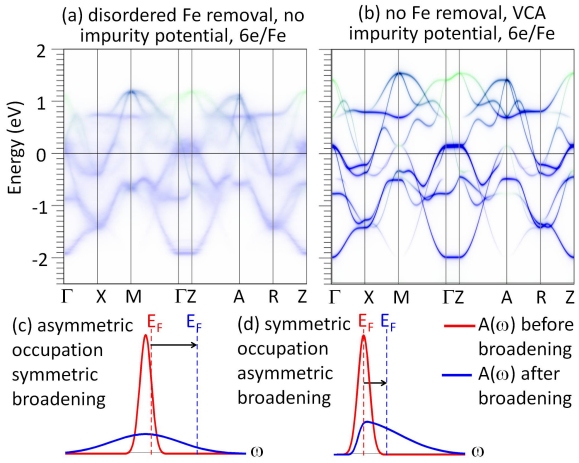

FIG. 2: (color online) Spectral function obtained from disordered removal of Fe orbitals alone (without the impurity potentials) (a), and from the virtual crystal of the impurity potentials (without the removal of Fe orbitals). Both show negligible effective doping in comparison with the full disordered calculation. (c)(d) Illustration of microscopic mechanisms contributing to effective doping through broadening in frequency.

Figure 2 illustrates two microscopic mechanisms that contribute to the effective doping through disorder induced broadenings in frequency. For simplicity, let's consider the broadening of the momentum independent spectral function $A(\omega)$. First, in Fig. 2(c), when the spectral weight near the chemical potential (within the frequency

range of the broadening) is larger below, a symmetric broadening in frequency pushes the chemical potential up. Second, in Fig. 2(d), an asymmetric broadening skewed toward higher frequency alone does the same [26]. Figure 3(c) illustrates a clear asymmetric spectral function contributing to raise the chemical potential. Since the large chemical potential shift only takes place upon including disordered repulsive impurity potential at Se atoms, the asymmetric broadening must originate from the same. A microscopic explanation of such asymmetric broadening is given in the supplementary materials [21].

Without increasing the total electronic density of the system, the significant shift of chemical potential leads to many important physical consequences through, for example, the change of Fermi velocity and the Fermi wave vector, in a manner similar to real doping in regular systems without disorder. In particular, the significant suppression of phase space for long-range magnetic order around (π,0) resembles very much the effect of real doping. This offers a natural explanation of the occurrence of a superconducting phase in this undoped system, and suggests a novel mechanism of promoting superconductivity via strongly disordered impurity potentials.

Interestingly, there have indeed been experimental observations suggesting enhancement of superconductivity via disorder in these systems. Reference [27] reported that the same sample can be made superconducting/magnetically ordered through quenching/annealing. High pressure experiments [28] reported a seemingly second superconducting transition at considerably higher temperature $T_c = 48K$ at pressure above 11.5GPa, consistent with promotion of superconductivity via pressure-induced suppression of vacancy order. A second superconducting phase has also been recently reported at ambient pressure [29].

Obviously, for disordered impurities to promote superconductivity, their positive influence (from the above effective doping or other disorder effects discussed below) must overcome the negative influence of disorder (for example pair-breaking or phase fluctuation scattering). This issue is intimately tied to the nature of the scatterer (for example, magnetic or nonmagnetic, weak scattering or strong scattering regime, and so on) and the superconductivity itself (for example, sign changing order parameter or not, dominant amplitude fluctuation or phase fluctuation, and so on). We anticipate rich physics to be revealed from future quantitative investigations along this direction.

It is also important to account for the removal of Fe orbitals in the vacancy sites. Indeed, representing the spectral function $A_j(k,\omega)$ in the eigenbasis $|kj\rangle$ of crystal momentum k and band index j of the uniform 122 system [23], Fig. 3 shows that the total spectral weights of all well-defined low-energy quasi-particle drop to ~0.8, in good accordance to the 20% Fe vacancy. As advocated previously [23], such a large reduction in the spectral weight is expected to change strongly (even qualitatively) the standard picture of spin fluctuations [30, 31], through a significant reduction of the bare susceptibility by roughly a factor of $0.8^2 \sim 0.6$. The general argument [23] of suppression/resilience of phase space of antiferromagnetic/superconducting order should remain valid, which leads to a potential promotion of superconductivity.

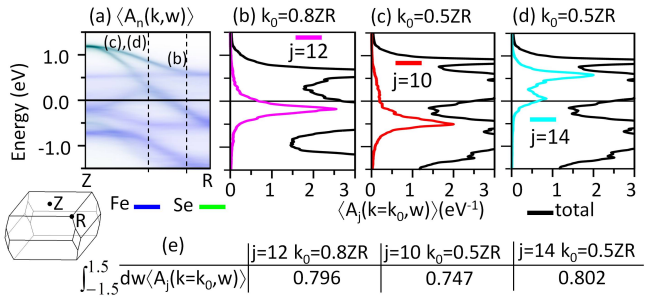

FIG. 3: (color online) Disorder induced spectral weight distributions, represented in the 2-Fe Brillouin zone, (a) as a function of crystal momentum k and orbital indices n, and at fixed crystal momenta k_0 and band index j with (b) $k_0 = 0.8$ZR and $j = 12$ belonging to the large electron pocket in the zone corner, (c) $k_0 = 0.5$ZR and $j = 10$ belonging to the hole pocket leaking into the Fermi surface, (d) $k_0 = 0.5$ZR and $j = 14$ displaying an incoherent satellite at the Fermi surface and (e) their integrations displaying ~20% loss of spectral weight due to the Fe vacancies.

In addition, our result reveals strong incoherent features in this system. For example, Fig. 3(c) illustrates that small amount of diffusive hole carriers in the system are still present in this seemingly highly electron doped system, through the long tails of the hole bands. This suggest that hole carriers could still contribute to the effective pairing [31]. Similarly, Fig. 3(d) shows the presence of highly incoherent carriers right at the chemical potential, originating from the normally unoccupied band 0.5eV above the chemical potential. All of these strong effects illustrate vividly the rich physics induced by disorder, well beyond a simple modification of the band filling or dispersion.

Finally, it is important to clarify that our case study with fully disordered vacancies is meant to illustrate the general features of poorly ordered regions of the sample, for example, near the surface where diffusion of vacancies is easier, or in the vacancy disordered region of a phase separated sample. While the presence of vacancy ordered regions has been demonstrated experimentally [3, 4, 14, 15], previous DFT calculations [32–34] have established that these regions will open a magnetic gap, so they cannot contribute to the bands near the FS. In principle, within the poorly ordered regions, the vacancies might tend to short-range ordered (SRO), given their charged nature. Furthermore, additional scattering related to short-range magnetic and orbital correla-

tion [35, 36] should also be present. These complications in real materials may modify the broadening quantitatively, but should not change our conclusions qualitatively.

In conclusion, we studied from first-principles the normal state configuration-averaged spectral function $\langle A(k,\omega)\rangle$ of $K_{0.8}Fe_{1.6}Se_2$ with disordered vacancies. We found that strong vacancy disorder does not destroy the band structure and Fermi surface, but is able to suppress the significant band structure reconstruction expected in vacancy ordered systems, thus producing the smooth quasi-particle band structure observed by ARPES. Furthermore, we found an intriguing disorder-induced "effective doping" that enlarges significantly the electron pockets to be comparable to the highly electron doped KFe_2Se_2, in excellent agreement with ARPES observations. Our result demonstrates clearly the general inapplicability of Luttinger theorem in disordered systems, and suggests that the region to which ARPES measurements are sensitive might be almost undoped after all, but with strong vacancy disorder. Finally, the observed effective doping, together with a strong ($\sim$20%) loss of coherent spectral weight, offers a novel, general mechanism to promote superconductivity in the presence of strong impurity potentials, as indicated by several current experiments.

Work funded by the U S Department of Energy, Office of Basic Energy Sciences DE-AC02-98CH10886 under the CMCSN program.

[1] J. Guo *et al.*, Phys. Rev. B **82**, 180520(R) (2010).
[2] M.-H. Fang *et al.*, Europhy. Lett. **94**, 27009 (2011).
[3] W. Bao *et al.*, Chinese Phys. Lett. **28**, 086104 (2011).
[4] F. Chen *et al.*, Phys. Rev. X **1**, 021020 (2011).
[5] X.-P. Wang *et al.*, Europhy. Lett. **93**, 57001 (2011).
[6] Y. Zhang *et al.*, Nat. Mater. **10**, 273 (2011).
[7] L. Zhao *et al.*, Phys. Rev. B **83**, 140508(R) (2011).
[8] D. Mou *et al.*, Phys. Rev. Lett. **106**, 107001 (2011).
[9] T. Qian *et al.*, Phys. Rev. Lett. **106**, 187001 (2011).
[10] S. V. Borisenko *et al.*, arXiv:1204.1316 (2012).
[11] I. I. Mazin *et al.*, Phys. Rev. Lett. **101**, 057003 (2008).
[12] W. Li *et al.*, Nat. Phys. **8**, 126 (2012).
[13] Y. Texier *et al.*, arXiv:1203.1834 (2012).
[14] Y. J. Yan *et al.*, Sci. Rep. **2**, 212 (2012).
[15] Z. Wang *et al.*, Phys. Rev. B **83**, 140505(R) (2011).
[16] A. Iadecola *et al.*, J. Phys. Condens. Matter **24**, 115701 (2012).
[17] C.-H. Lin *et al.*, Phys. Rev. Lett. **107**, 257001 (2011).
[18] W. Ku *et al.*, Phys. Rev. Lett. **89**, 167204 (2002)
[19] W. Ku, T. Berlijn and C.-C. Lee, Phys. Rev. Lett. **104**, 216401 (2010).
[20] T. Berlijn, D. Volja and W. Ku, Phys. Rev. Lett. **106**, 077005 (2011).
[21] Supplementary material.
[22] M. W. Haverkort, I. S. Elfimov and G. A. Sawatzky, arXiv:1109.4036.
[23] T. Berlijn *et al.*, arXiv:1112.4858 (2011).
[24] K. Nakamura, R. Arita and H. Ikeda., Phys. Rev. B **83**, 144512 (2011).
[25] S. Konbu *et al*, J. Phys. Soc. Jpn. **80**, 123701 (2011).
[26] These two mechanisms probably also contribute in the toy model study in Ref. [22].
[27] F. Han *et al.*, arXiv:1103.1347 (2011).
[28] L. Sun *et al.*, Nat. **483**, 67 (2012).
[29] A. M. Zhang *et al.*, arXiv:1203.1533 (2012).
[30] T. A. Maier *et al.*, Phys. Rev. B **83**, 100515(R) (2011).
[31] F. Wang *et al.*, Europhy. Lett. **93**, 57003 (2011).
[32] C. Cao and J. Dai, Phys. Rev. Lett. **107**, 056401 (2011).
[33] X.-W. Yan *et al.*, Phys. Rev. B **83**, 233205 (2011).
[34] X. -W. Yan *et al.*, Phys. Rev. Lett. **106**, 087005 (2011).
[35] Chi-Cheng Lee, Wei-Guo Yin, and Wei Ku, Phys. Rev. Lett. **103**, 267001 (2009).
[36] S. Liang *et al.*, arXiv:1111.6994 (2012).